Paul Arras, Jasmin Zimmermann, Britta Lipinski, Bernhard Valldorf, Andreas Evers, Desislava Elter, Simon Krah, Achim Doerner, Enrico Guarnera, Vanessa Siegmund, Harald Kolmar, Lukas Pekar and Stefan Zielonka*

Bovine ultralong CDR-H3 derived knob paratopes elicit potent TNF-α neutralization and enable the generation of novel adalimumab-based antibody architectures with augmented features

https://doi.org/10.1515/hsz-2023-0370
Received December 14, 2023; accepted January 29, 2024;
published online February 20, 2024

Abstract: In this work we have generated cattle-derived chimeric ultralong CDR-H3 antibodies targeting tumor necrosis factor α (TNF-α) *via* immunization and yeast surface display. We identified one particular ultralong CDR-H3 paratope that potently neutralized TNF-α. Interestingly, grafting of the knob architecture onto a peripheral loop of the CH_3 domain of the Fc part of an IgG1 resulted in the generation of a TNF-α neutralizing Fc (Fc_{knob}) that did not show any potency loss compared with the parental chimeric IgG format. Eventually, grafting this knob onto the CH_3 region of adalimumab enabled the engineering of a novel TNF-α targeting antibody architecture displaying augmented TNF-α inhibition.

Keywords: antibody display; antibody engineering; antibody valency; biparatopic antibody; bovine ultralong CDR-H3 antibody; Fc_{knob}

1 Introduction

A subset of antibodies found in cattle harbors ultralong CDR-H3 regions of up to 70 amino acids that form a protruding paratope (Haakenson et al. 2018; Saini et al. 1999). From a structural perspective, these peculiar paratopes typically adopt a very similar structure consisting of a stalk region that is composed of an ascending as well as descending β-strand and the knob domain (Wang et al. 2013). The knob domain which is primarily responsible for antigen binding, displays a vast structural diversity due to the presence of different disulfide bond patterns (Dong et al. 2019). These disulfide bonds rigidify the paratope and are critical for antigen binding (Svilenov et al. 2021). The main function of the stalk region relies in mediating structural stability (Passon et al. 2023; Svilenov et al. 2021) and it was demonstrated by Smider and co-workers that mutations within this architecture might impede the functionality of the paratope to a certain degree (Stanfield et al. 2020). Notwithstanding, Macpherson and co-workers were able to chemically synthesize a solitary knob architecture by solid-phase peptide synthesis, proving that the presence of a stalk region is not an absolute requirement for the knob paratope to function adequately (Macpherson et al. 2021a).

Since as of now the knob-based paratope represents the smallest antibody-derived paratope that can be harnessed by immunization. Most recently, efforts were made to

***Corresponding author: Stefan Zielonka**, Antibody Discovery & Protein Engineering, Merck Healthcare KGaA, Frankfurter Straße 250, D-64293 Darmstadt, Germany; and Biomolecular Immunotherapy, Institute for Organic Chemistry and Biochemistry, Technische Universität Darmstadt, Peter-Grünberg-Strasse 4, D-64287 Darmstadt, Germany, E-mail: Stefan.zielonka@merckgroup.com. https://orcid.org/0000-0002-4649-2843
Paul Arras, Antibody Discovery & Protein Engineering, Merck Healthcare KGaA, Frankfurter Straße 250, D-64293 Darmstadt, Germany; Biomolecular Immunotherapy, Institute for Organic Chemistry and Biochemistry, Technische Universität Darmstadt, Peter-Grünberg-Strasse 4, D-64287 Darmstadt, Germany; and Targeted mRNA Delivery, Merck KGaA, Frankfurter Straße 250, D-64293 Darmstadt, Germany
Jasmin Zimmermann, **Andreas Evers**, **Desislava Elter**, **Simon Krah**, **Achim Doerner**, **Enrico Guarnera and Lukas Pekar**, Antibody Discovery & Protein Engineering, Merck Healthcare KGaA, Frankfurter Straße 250, D-64293 Darmstadt, Germany. https://orcid.org/0000-0003-4643-1941 (A. Evers). https://orcid.org/0000-0001-9259-0965 (L. Pekar)
Britta Lipinski, Antibody Discovery & Protein Engineering, Merck Healthcare KGaA, Frankfurter Straße 250, D-64293 Darmstadt, Germany; and Biomolecular Immunotherapy, Institute for Organic Chemistry and Biochemistry, Technische Universität Darmstadt, Peter-Grünberg-Strasse 4, D-64287 Darmstadt, Germany
Bernhard Valldorf, Targeted mRNA Delivery, Merck KGaA, Frankfurter Straße 250, D-64293 Darmstadt, Germany
Vanessa Siegmund, Early Protein Supply & Characterization, Merck Healthcare KGaA, Frankfurter Straße 250, D-64293 Darmstadt, Germany
Harald Kolmar, Applied Biochemistry, Institute for Organic Chemistry and Biochemistry, Technische Universität Darmstadt, Peter-Grünberg-Strasse 4, D-64287 Darmstadt, Germany. https://orcid.org/0000-0002-8210-1993

generate antigen-specific knobs. It was first shown by Macpherson and co-workers that autonomous knob paratopes can be generated in a sophisticated process involving ultralong CDR-H3 Fab expression followed by tobacco etch virus-mediated cleavage and release of the knob domain (Macpherson et al. 2020). In addition, our group engineered knob-Fc fusion proteins, referred to as Knobbodies (Pekar et al. 2021b). Interestingly, in this study, only a fraction of knob regions that were functional within the natural Fab context were adequately produced as Knobbodies. In addition to this, Knobbodies were reduced in their binding capacities compared to their parental Fabs. While affinities were fairly equal between knob-Fc fusions and their IgG counterparts, cellular binding capacities as well as killing capacities *via* antibody-dependent cell-mediated cytotoxicity (ADCC) were diminished. Remarkably, this is in line with findings of Smider and co-workers who produced independent knob paratopes targeting SARS-CoV2 as TrxA-knob constructs in *Escherichia coli* followed by enterokinase cleavage of TrxA functioning as chaperone (Huang et al. 2023). While binding affinities were largely retained, neutralization potencies were significantly diminished for the independent knob domains compared with the parental Fab counterparts.

Besides exploiting the knob as solitary antigen binding unit, this miniprotein was also utilized as building block for the generation of more sophisticated multifunctional antibody derivatives. Our group recently demonstrated that the ultralong CDR-H3 repertoire in cattle can be readily harnessed for the generation of bispecific antibodies (Klewinghaus et al. 2022). Due to the underlying specific genetics of bovine ultralong CDR-H3 antibodies – ultralong CDR-H3 heavy chains typically pair with a single VL gene that is reasonably sequence conserved (Dong et al. 2019; Stanfield et al. 2016, 2020; Wang et al. 2013) – this specific repertoire can be contemplated as almost natural source of common light chain bispecifics (Krah et al. 2018). Additionally, Hawkins et al. implanted antigen-specific knob domains into rat serum albumin as well as into a CDR-distal loop of a VHH domain, enabling the facile implementation of a novel binding specificity into a protein with a predefined function, resulting in bifunctional molecules (Hawkins et al. 2022). This approach was lately broadened by the same group by virtue of grafting albumin binding knob domains onto the VH framework III loop for the generation of bispecific Fab fragments with extended pharmakokinetics (Adams et al. 2023). Most recently, our group has shown that target specific knob paratopes can also be grafted onto peripheral loops (AB and EF) of the CH_3 domain of the Fc region of IgG1, enabling the generation of a novel symmetric bispecific antibody format (Yanakieva et al. 2023). Essentially, Fc-mediated effector function were not significantly impeded.

TNF-α is a pleiotropic and proinflammatory cytokine that is generally considered as one of the main mediators in the pathogenesis of autoimmune inflammatory diseases (Li et al. 2017; Moudgil and Choubey 2011). Consequently, several different inhibitors of TNF-α were granted marketing approval for disease treatment, such as infliximab, etanercept, certolizumab pegol or golimumab (Jang et al. 2021). In this regard, adalimumab, a fully human IgG1 blocking the interaction of TNF-α to its cognate receptors has proven to be of utmost relevance in terms of both, therapeutic efficacies as well as commercial performance (Figure 1A) (Bain and Brazil 2003; Urquhart 2023).

In this work, we have generated TNF-α specific bovine ultralong CDR-H3 paratopes by combining animal immunization with yeast surface display. Interestingly, when reformatted as chimeric bovine x human IgG (Figure 1B), one particular paratope elicited quite strong neutralization of TNF-α. For further characterization, we engineered the Knobbody counterpart (Figure 1C) derived from this ultralong CDR-H3 paratope as well as Fc_{knob} variants, by engrafting the respective knob region onto the AB loop or EF loop of the CH_3 domain of the Fc region (Figure 1D). Essentially, grafting the knob domain onto the peripheral loops (AB or EF) of the CH_3 domain of adalimumab enabled the construction of a novel tetravalent antibody architecture with significantly enhanced neutralization capacities (Figure 1E).

2 Results

2.1 Yeast surface display enables the isolation of TNF-α specific ultralong CDR-H3 paratopes

We have previously described a platform process for specifically harnessing the bovine ultralong CDR-H3 repertoire by combining animal immunization with yeast surface display (Pekar et al. 2021b).

The same procedure was applied for the generation of TNF-α targeting ultralong paratopes. In brief, two cattle were immunized with recombinant human (rh) TNF-α. Following immunization, based on the peripheral blood mononuclear cell (PBMC) repertoire and RNA as well as cDNA derived therefrom, the ultralong CDR-H3 repertoire encoding for the stalk and knob architectures was specifically amplified by PCR. To this end, forward primers were exploited which specifically annealed at the 3′ nucleotide

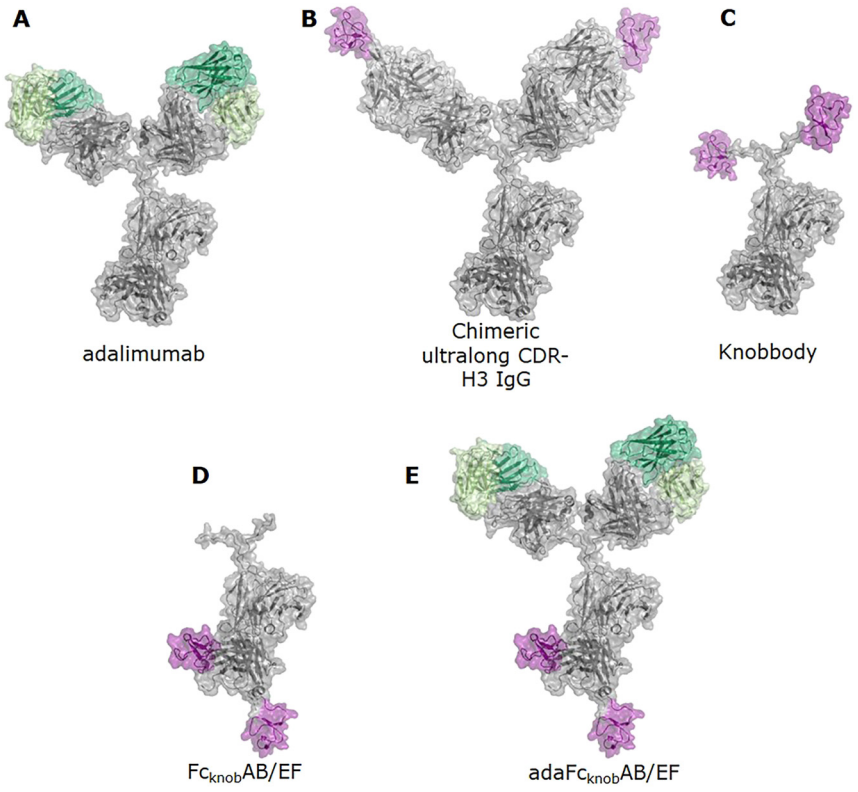

Figure 1: Structural models of generated anti-TNF-α antibodies. Architectures of tested molecule formats based on anti-TNF-α Fab (green) and cattle-derived ultralong CDR-H3 knob (magenta) assessed for their ability to neutralize TNF-α in functional assays. Depiction of adalimumab (A) and chimeric ultralong CDR-H3 IgG (B) antibodies as well as engineered formats thereof. Ultralong CDR-H3 engraftment onto human IgG Fc portion is indicated as format C (Knobbody), while introduction of knob structure into CH3 AB or EF peripheral loop structures ($Fc_{knob}AB/EF$) is shown as format D. Combination of adalimumab with knob CH3 AB/EF engraftment ($adaFc_{knob}AB/EF$) is indicated as format E. Schemes were generated using PyMol software version 2.3.0.

extension of IGHV1-7 (also referred to as VHBUL) as well as reverse primers annealing to framework region 4 (FR4) as described elsewhere (Arras et al. 2023c). Based on this diversity, a chimeric (*bovine* × *human*) Fab library was constructed in a process involving homologous recombination (gap repair cloning (Benatuil et al. 2010)) followed by yeast mating (Roth et al. 2019; Weaver-Feldhaus et al. 2004), giving rise to diploid cells and consequently allowing for functional chimeric Fab display. Essentially, the constructed library with a size of approximately 6×10^7 unique clones was subjected for library sorting by employing fluorescence activated cell sorting (FACS). For this, an antigen concentration of 1 µM was used. To co-select for functional Fab display besides the binding functionality, we applied a two-dimensional staining strategy involving a detection antibody binding to the constant region of the λ light chain. As shown in Figure 2 we were able to significantly enrich for a (rh) TNF-α binding population within three rounds of FACS sorting (Figure 2). Sequencing unveiled 77 unique ultralong CDR-H3 regions. Within this set, clonotyping was performed by evaluating sequence distances, setting a threshold of >97 % CDR-H3 sequence identity (approximately a 2-residue difference) which resulted into 26 sequence clusters. The overall similarity between these clusters exhibited great variation, with a sequence identity of only 38.5 % on average.

2.2 A subset of bovine × human chimeric ultralong CDR-H3 IgG antibodies significantly neutralize TNF-α

For antibody production, we nominated these 26 ultralong CDR-H3 paratopes that were reformatted and produced as *bovine* × *human* IgG1 antibodies harboring bovine variable domains followed by human constant regions (Figure 1B). Expression yields were in the double-digit milligram per liter scale, indicating adequate production profiles in general (Supplementary Table 1). Likewise, besides several outliers, size exclusion chromatography (SEC) target peaks post protein A purification were above 85 % for most of generated ultralong CDR-H3 antibodies. As (rh) TNF-α is a trimeric molecule and the generated chimeric bovine × human ultralong CDR-H3 IgGs were produced as bivalent antibodies, fine determination of affinities was not possible in a biolayer interferometry (BLI) setting. Consequently, we only performed qualitative binding experiment at a single (rh) TNF-α concentration of 100 nM (Supplementary Figure 1) and focused on determination of the biological functionality i.e. neutralization capacities. However, eleven out of 26 chimeric antibodies showed specific binding to (rh) TNF-α as determined by BLI. Those were scrutinized more meticulously in terms of their TNF-α inhibition potential by exploiting TNF-α reporter cells which produce a secreted

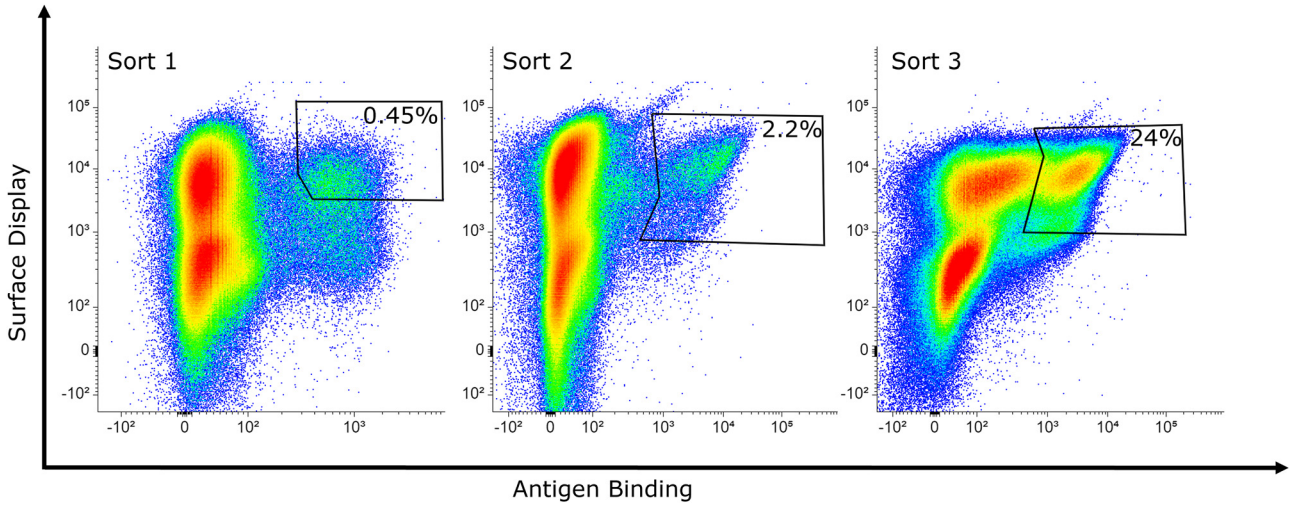

Figure 2: Yeast surface display enables the isolation of anti-TNF-α antibodies. FACS-based enrichment of the ultralong CDR-H3 library by applying a two-dimensional sorting strategy for simultaneous detection of (rh) TNF-α binding and Fab display. Dot plots show representative 10^6 cells of the three conducted sorting rounds employing 1 μM of antigen, respectively. Applied sorting gates and corresponding cell population (as % of total cells) are shown.

embryonic alkaline phosphatase reporter gene upon stimulation with (rh) TNF-α (HEK-Blue™ TNF-α cells). In this setup, reporter cell activation of 1 ng per ml (rh) TNF-α was assessed in the presence or absence of TNF-α targeting chimeric ultralong CDR-H3 molecules at two fixed concentrations, 25 and 5 nM, respectively (Figure 3). As expected, adalimumab which was exploited as positive control elicited potent neutralization of (rh) TNF-α at both concentrations tested. In contrast to this, most of the generated ultralong CDR-H3 antibodies did not neutralize (rh) TNF-α, despite binding to this cytokine in a specific manner. Nevertheless, several clones (e.g., B.16 or B.17), showed trends towards weak (rh) TNF-α inhibition with ultralong CDR-H3 IgG B.25 and B.26 triggering statistically significant neutralization at the higher concentration of 25 nM. Interestingly, one particular ultralong CDR-H3 antibody (clone B.01) robustly neutralized (rh) TNF-α at both dose levels tested. Clone B.01 harbored a CDR-H3 region encompassing 62 aminos acids and six Cys residues. The knob paratope (without stalk regions) comprised 44 amino acids (sequence given in Supplementary Figure 2). This molecule was considered for further engineering and characterization. In this respect, we aimed at investigating the targeted epitope of B.01 in direct comparison to adalimumab. For this, an epitope binning experiment was conducted using BLI in which (rh) TNF-α was captured followed by two consecutive association steps with B.01 followed by adalimumab. As control, adalimumab or B.01 was exploited for both steps (Supplementary Figure 3). Compared to the controls, a second association was observed for adalimumab after binding of B.01 under saturating conditions. However, the interference pattern shift was clearly diminished in contrast to association of adalimumab to (rh) TNF-α only, indicating either an overlapping but not identical epitope that were addressed by B.01 and adalimumab or epitopes in close proximity resulting into steric hindrance.

2.3 Engineering of an adalimumab derived antibody architecture with augmented inhibition capacities by grafting an ultralong CDR-H3 knob paratope onto the Fc region

We have previously described the generation of Knobbodies, in which the knob region of ultralong CDR-H3 regions is directly grafted onto the hinge region followed by the Fc portion (Pekar et al. 2021b). To further characterize whether the 44 amino acid comprising knob domain of ultralong CDR-H3 antibody B.01 autonomously functions as paratope enabling efficient TNF-α neutralization, we generated a Knobbody derived thereof (Figure 1C). In addition, we constructed Fc_{knob} versions of B.01, in which the knob architecture was either grafted onto the peripheral AB or EF loop of the CH3 region of the Fc part (Figure 1D). This novel antibody format has recently been described by our group (Yanakieva et al. 2023). Herein, the knob domain is flanked on both termini with a Gly4Ser linker and either replaces the EEMTK motif of the AB loop or the DKS motif of the EF loop of the CH3 region, respectively. Finally, in order to investigate if the knob derived from B.01 enables the

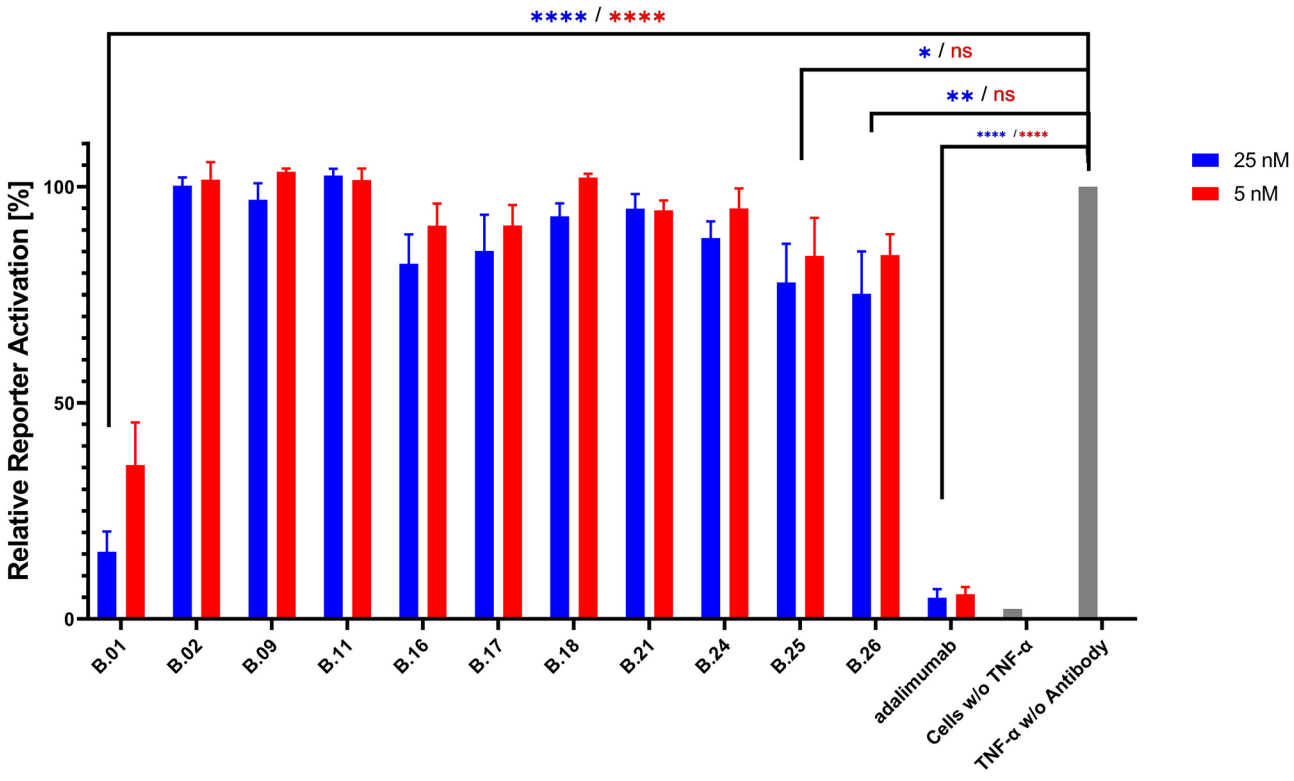

Figure 3: Cattle-derived ultralong CDR-H3 antibodies mediate (rh) TNF-α neutralization *in vitro*. Initial assessment of the capabilities of a set of *bovine* × *human* ultralong CDR-H3 antibodies to inhibit (rh) TNF-α (at 1 ng/mL) mediated activation of HEK-Blue™ TNF-α sensitive reporter cells. Graph shows mean relative reporter activation ± SEM for two antibody concentrations (25 nM shown in blue and 5 nM shown in red) of two independent experiments. *$p \leq 0.05$, **$p \leq 0.01$, ***$p \leq 0.001$, ****$p \leq 0.0001$, ns: not significant (compared to TNF-α treatment only). Of note, adalimumab was produced harboring an effector silenced Fc region.

construction of a novel version of adalimumab with enhanced neutralization potencies, we also grafted this respective knob onto the CH_3 AB or EF loop of Adalimumab (Figure 1E). Of note, all sequences are given in Supplementary Figure 2. The different knob-based formats derived from B.01 were produced in Expi293™ cells. Expression yields were in the double digit milligram per liter scale and fairly similar to the production of adalimumab (Table 1). Except for the Knobbody version of B.01 (SEC target peak of 80.5 %), purities as determined by SEC following protein A purification were generally above 85 % target species, indicating adequate properties (Supplementary Figure 5). Furthermore, all different architectures showed specific binding to (rh) TNF-α, as determined by BLI (Supplementary Figure 4). Subsequently, all constructs were further assessed with respect to their neutralization capacities in a reporter cell assay using a broad concentration range (Figure 4A, HEK-Blue™ TNF-α cells). In this assay, adalimumab was quite potent in inhibiting (rh) TNF-α based stimulation of the reporter cells (IC_{50} = 0.095 nM), while chimeric ultralong CDR-H3 IgG (B.01) was attenuated in direct comparison (IC_{50} = 1.348 nM). In accordance with previously published data (Pekar et al. 2021b; Yanakieva et al. 2023), generating the Knobbody version resulted into compromised functionalities i.e., reduced potencies of (rh) TNF-α neutralization by approximately 27-fold (IC_{50} = 36.73 nM). This is in contrast to the construction of Fc_{knob} prototypes of B.01. Here, both, the AB loop as well as the EF loop engraftments of the B.01 knob paratope were quite similar to the IgG version in (rh) TNF-α neutralization (IC_{50} = 0.877 nM for Fc_{knob}AB and 2.973 nM for Fc_{knob}EF). Most importantly, when the Fc_{knob} architectures were incorporated into CH_3 domain of adalimumab, this resulted in augmented (rh) TNF-α inhibition. In this regard, the B.01 knob engraftment into the EF loop of the CH_3 domain of adalimumab only slightly optimized neutralization potencies (IC_{50} = 0.052 nM for adaFc_{knob}EF *vs.* 0.095 nM for adalimumab). The AB loop engraftment, however, considerably enhanced potencies in terms of (rh) TNF-α neutralization (IC_{50} = 0.006 nM for adaFc_{knob}AB). This is in line with target engagement assays (Supplementary Figure 4) revealing superior binding capacities especially for adaFc_{knob}AB. Here, the interference pattern shift (BLI) at a

fixed concentration of 100 nM was clearly increased for the B.01 derived knob engrafted onto the CH_3 domain of adalimumab compared to all other constructs including both parental molecules (adalimumab as well as B.01 IgG).

It is known that TNF-α elicits direct killing of various different cancer cell lines (Carswell et al. 1975; Dakhel et al. 2021). In another attempt to further analyze the different antibody architectures, we scrutinized the inhibition of TNF-α mediated killing of murine L929 cells (Humphreys and Wilson 1999). For this, killing was assessed at a (rh) TNF-α concentration of 10 nM. The different antibody-derived constructs were added at a concentration of 8 nM. As shown in Figure 4B, at this concentration, adalimumab only minorly inhibited killing of L929 cells triggered by TNF-α. Likewise, also ultralong CDR-H3 IgG B.01, the Knobbody based on B.01 as well as Fc_{knob} derivatives only slightly reduced TNF-α induced killing. On the contrary, adalimumab derived molecules with CH_3 engrafted knob domains $adaFc_{knob}AB$ as well as $adaFc_{knob}EF$ substantially inhibited TNF-α mediated killing of L929 cells. Eventually, this resulted into trends of enhanced potencies of inhibiting TNF-α mediated killing (IC_{50}) elicited by $adaFc_{knob}AB$ as well as $adaFc_{knob}EF$ (IC_{50} = 3.76 nM and 3.75 nM, respectively) compared to adalimumab (IC_{50} = 11.22 nM, Supplementary Figure 6). Taken together, these findings are giving clear evidence that TNF-α specific Fc_{knob} designs based on cattle-derived ultralong CDR-H3 paratopes can be exploited for the generation of novel adalimumab-based antibody formats with augmented features.

Table 1: Expression yields, SEC purities and (rh) TNF-α neutralization potencies of bovine × human chimeric antibody B.01 and adalimumab as well as engineered derivates Knobbody, $Fc_{knob}AB$, $Fc_{knob}EF$, $adaFc_{knob}AB$, $adaFc_{knob}EF$.

			HEK-Blue™ reporter cell	
	Yield (mg/l)	% Purity-SEC (%)	IC50 (nM) ± Std. error	R^2
Knobbody	60.1	80.5	36.73 ± 8.364	0.96
$Fc_{knob}EF$	78.0	95.3	2.973 ± 0.32	0.98
$Fc_{knob}AB$	75.8	87.4	0.877 ± 0.117	0.98
$adaFc_{knob}EF$	66.8	97	0.052 ± 0.008	0.98
$adaFc_{knob}AB$	75.6	97.4	0.006 ± 0.002	0.97
B.01	96.7	97.5	1.348 ± 0.681	0.96
Adalimumab	81.5	100	0.095 ± 0.014	0.98

Expression yields were determined after protein A purification. Purities were determined by analytical size exclusion chromatography post protein A purification. Neutralization potencies were assessed in a HEK-Blue™ reporter cell assay and are presented ± the standard error.

3 Discussion

In order to efficiently inhibit the proinflammatory cytokine TNF-α, we have generated and engineered antibody-derived architectures based on bovine ultralong CDR-H3 paratopes. TNF-α is a master regulator of inflammatory processes and consequently, multiple TNF neutralizing therapeutics have been approved for the treatment of autoimmune diseases (Jang et al. 2021; Li et al. 2017). To generate TNF-α inhibiting molecules, we immunized cattle with (rh) TNF-α. It is known since quite some time that the adaptive immune repertoire in cattle produces a subset of antibodies with peculiar long CDR-H3 regions of up to 70 amino acids (Haakenson et al. 2018; Saini et al. 2003, 1999). This set of antibodies has been efficiently harnessed to address several different antigens, such as viral components (Huang et al. 2023; Sok et al. 2017; Wang et al. 2013), complement proteins (Macpherson et al. 2021a, 2021b), serum albumin (Adams et al. 2023) or cellular receptors (Klewinghaus et al. 2022; Pekar et al. 2021b). Intriguingly, it was demonstrated that the main antigen-binding architecture of the CDR-H3, the knob region, can function as autonomous paratope (Huang et al. 2023; Macpherson et al. 2020), paving the way for a plethora of different engineering options (Adams et al. 2023; Hawkins et al. 2022; Macpherson et al. 2021a; Pekar et al. 2021b; Yanakieva et al. 2023).

From the PBMC repertoire of immunized cattle we were able to specifically enrich for TNF-α targeting ultralong CDR-H3 antibodies by yeast surface display (Doerner et al. 2014; Valldorf et al. 2022). Within the set of eleven sequence diverse IgGs (Figure 1B), only one particular clone (B.01) enabled a robust inhibition of TNF-α in a reporter cell assay. Compared with adalimumab which is from a commercial perspective one of the most successful biotherapeutics to this date (Urquhart 2023), neutralization potencies were reduced by approximately 14-fold. In a recent study that was inspired by work conducted by Rüker and co-workers (Wozniak-Knopp et al. 2010), our group was able to show that antigen-specific knob domains can be grafted onto peripheral loops of the CH_3 domain of an IgG, giving rise to a novel symmetric bispecific antibody format (Yanakieva et al. 2023). To investigate whether the TNF-α neutralizing knob derived of B.01 can also function in an autonomous manner, we grafted this domain onto the AB loop as well as onto the EF loop of the CH_3 domain of an effector silenced Fc domain (Fc_{knob}, Figure 1D). In addition, we also engineered the Knobbody version of B.01 (Figure 1C), in which the knob domain is fused onto the hinge region of the Fc part (Pekar et al. 2021b). In accordance with previous findings (Pekar et al. 2021b; Yanakieva et al. 2023), while still

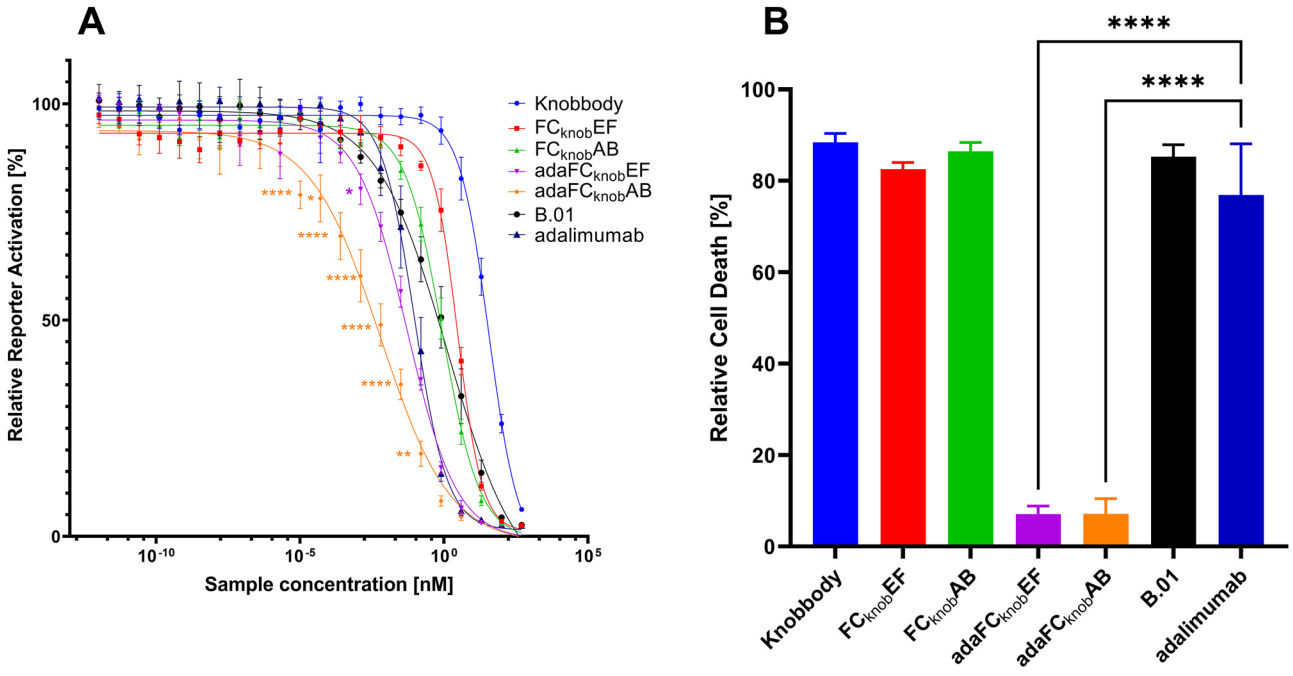

Figure 4: Cattle-derived ultralong CDR-H3 knob based antibodies mediate dose dependent neutralization of TNF-α and augment inhibitory capacities of adalimumab. Assessment of inhibitory capacities of bovine × human chimeric antibody B.01 and Fc-silenced adalimumab as well as engineered derivates (A) on HEK-Blue™ TNF-α reporter cells (rh TNF-α at 1 ng/ml) and in an orthogonal cytotoxicity assay (B) using TNF-α susceptible L929 cells (antibody samples at 8 nM and rh TNF-α at 10 nM). Dose response curves ±SEM were calculated using a non-linear regression variable slope four parameter fit from at least three independent experiments. Sample points were compared using an ordinary one-way ANOVA with Dunnett's multiple comparisons test. *$p \leq 0.05$, **$p \leq 0.01$, ****$p \leq 0.0001$ (compared to (A) adalimumab or (B) TNF-α treatment only).

efficiently neutralizing TNF-α in a reporter cell assay at high concentrations, potency of the Knobbody version of B.01 was significantly attenuated compared to the parental IgG (by approximately 27-fold). This is in stark contrast to the Fc$_{knob}$ versions of B.01 which demonstrated quite similar potencies in inhibiting TNF-α mediated reporter cell activation in comparison to the parental IgG.

From epitope binning experiments we were able to deduce that B.01 most likely targets an overlapping but non-identical epitope compared to adalimumab or an epitope in close proximity. Consequently, we set out to investigate whether biparatopic versions of adalimumab with higher valencies by constructing Fc$_{knob}$ version of adalimumab (adaFc$_{knob}$, Figure 1E) would result in augmented neutralization potencies. Strikingly, especially B.01 engrafted onto the AB loop of the CH3 domain of adalimumab (adaFc$_{knob}$AB) was significantly more potent in neutralizing TNF-α compared to adalimumab alone. In this respect, the IC$_{50}$ in TNF-α was optimized by more than 15-fold. These findings were further substantiated in a TNF-α based killing assay of L929 cells. At a fixed antibody concentration of 8 nM, adalimumab only moderately inhibited killing of L929 cells, whereas both engineered adaFc$_{knob}$ versions robustly neutralized killing capacities of TNF-α. To the best of our knowledge, we were able to demonstrate for the first time that ultralong CDR-H3 regions can be exploited for the neutralization of proinflammatory cytokines and most importantly that cattle-derived knob domains can be harnessed to create novel versions of pre-existing therapeutic antibodies with augmented features. Notwithstanding, the foreign nature of the knob domain might pose a substantial issue in terms of immunogenicity when administered to patients. In contrast to camelid-derived VHH domains that have been proven to be versatile for biomedical applications (Duggan 2018; Keam 2023; Markham 2022) and that can be readily humanized in different ways (Arras et al. 2023b, 2023a; Rossotti et al. 2022; Sulea 2022; Vincke et al. 2009), it remains to be determined whether cattle-derived knob paratopes can be sufficiently humanized.

4 Materials and methods

4.1 Cattle immunization

Two female cattle (*Bos taurus*) were immunized with (rh) tumor necrosis factor alpha (TNF-α, AcroBiosystems) at preclinics GmbH, Germany. All experimental procedures and animal care adhered to local

laws and regulations for animal welfare. Briefly, each immunization involved the subcutaneous administration of 400 µg TNFα, dissolved in 2 mL phosphate buffered saline (PBS), and mixed with 2 mL of Fama adjuvant (GERBU Biotechnik). Injections were performed at multiple sites. A total of six immunizations were conducted over 84 days (on days 0, 28, 42, 56, 70, and 84). On day 88, 100 ml of whole blood was collected from both animals, followed by the extraction of total RNA and subsequent complementary DNA (cDNA) synthesis.

4.2 Yeast surface display library generation

The detailed protocol for library construction involving strains, reagents, and plasmids has been previously described (Arras et al. 2023c; Klewinghaus et al. 2022; Pekar et al. 2021b). In brief, Saccharomyces cerevisiae strain EBY100 MATa (URA3-52 trp1 leu2Δ1 his3Δ200 pep4::HIS3 prb1Δ1.6R can1 GAL (pIU211:URA3)) was employed for generating the heavy chain diversity, while BJ5464 cells (MATα URA3-52 trp1 leu2Δ1-his3D200 pep4::HIS3 prb1Δ1.6R can1 GAL) containing the light chain plasmid (pLC) encoding a specific VLλ30 were utilized. Primer sets for specific ultralong CDR-H3 amplification can be found elsewhere (Arras et al. 2023c; Pekar et al. 2021b). PCR-based amplification involved using 1 µl of cDNA pooled from both specimens in a final volume of 50 µl with 0.5 µM of forward and reverse primers, respectively, along with Q5 High-Fidelity 2× Master Mix (New England Biolabs; NEB). The amplification conditions were as follows: 98 °C for 3 min, 35 cycles of 30 s at 98 °C and 50 s at 72 °C, followed by a final DNA elongation step for 2 min at 72 °C. PCR products were purified using the Wizard® SV Gel and PCR Cleanup System (Promega).

For library construction, gap repair cloning, following the method of Benatuil and colleagues was employed (Benatuil et al. 2010). In each electroporation reaction we used 12 µg of CDR-H3 PCR product and 4 µg of BsaI-HF (New England Biolabs) digested heavy chain destination plasmid (pHC). The estimated library size was determined by dilution plating on SD-Trp agar plates. To achieve Fab display, EBY100 cells containing the heavy chain diversity and BJ5464 cells with the single light chain were combined through yeast mating (Weaver-Feldhaus et al. 2004).

4.3 Yeast surface display library sorting

For library sorting, cells were cultured overnight in SD-Trp-Leu medium at 30 °C and 120 rpm. Afterwards, cells were harvested by centrifugation and used to inoculate SG-Trp-Leu medium at an OD_{600} of 1.0, followed by incubation for 2 days at 20 °C. Fab expression was detected by incubating with a light chain-specific goat F(ab')2 anti-human lambda R-phycoerythrin (R-PE) during the initial sorting round, or conjugated with Alexa Fluor 647 for subsequent enrichments (both from SouthernBiotech, diluted 1:20). Simultaneous staining for antigen binding was carried out using Penta-His Alexa Fluor 647 conjugate antibody (Qiagen, diluted 1:20) for sorting round 1 or Anti-6X His tag® PE antibody (Abcam, diluted 1:40) for sorting rounds 2 and 3. For this, cells were harvested, washed twice with PBS (Sigma Aldrich) and incubated with (rh) TNF-α at a concentration of 1 µM for 30 min on ice. After three washing steps, cells were incubated with secondary labeling reagents for an additional 30 min on ice. Subsequently, cells were again washed thrice with PBS and resuspended in an appropriate volume for FACS sorting using a BD FACSAria™ Fusion cell sorter (BD Biosciences).

DNA of the enriched yeast library was purified using the MasterPure Yeast DNA Purification Kit (Lucigen) and transformed into electrocompetent *E. coli* Top 10 (Inivitrogen) according to the manufacturer's manual. 192 clones were picked from LB-amp agar plates and sent for Sanger sequencing (Microsynth). Analysis of the sequencing histograms and clonotyping was performed with Geneious Prime® 2021.1.1.

4.4 Antibody expression and purification

For antibody expression, the pTT5 vector system was employed (Durocher 2002). Chimeric *bovine* × *human* IgGs as well as adalimumab and engineered derivatives were expressed using a Fc effector silenced backbone (Pekar et al. 2021a). The B.01-derived Knobbody and Fc_{knob} engraftments as well as adaFc_{knob} derivatives were constructed as described elsewhere (Pekar et al. 2021b; Yanakieva et al. 2023). Sequences are given in Supplementary Figure 2. All proteins were expressed in a volume of 5 ml using the ExpiCHO™ expression system (Thermo Fisher Scientific) or at 25 ml scale harnessing Expi293™ cells (Thermo Fisher Scientific) according to the manufacturers manual, employing a 2:1 ratio for the heavy chain and light chain, respectively. After 7 days the protein containing supernatants were purified exploiting MabSelect™ antibody purification chromatography resin (Cytiva). After sterile filtration, protein concentrations were determined by A_{280} absorption measurement. For the assessment of protein sample quality regarding monomer content [%], analytical size exclusion chromatography (SEC) was applied using 7.5 µg protein per sample on a TSKgel UP-SW3000 column (Tosoh Bioscience).

4.5 Biolayer interferometry

To evaluate the binding capacities of all cattle-derived proteins to (rh) TNF-α, we employed the Octet RED96 system (ForteBio, Pall Life Science) with 1000 rpm agitation at 25 °C. Initial confirmation of binding of the different antibodies and antibody architectures involved loading at 3 µg/mL in PBS for 180 s on anti-human Fc (AHC2) biosensors, followed by a 60 s sensor rinsing step in PBS. The subsequent association with (rh) TNF-α was measured for 180 s using 100 nM of the antigen.

For the investigation of potential epitope overlap between the cattle-derived clone B.01 and adalimumab, a competition analysis was conducted. Each protein was loaded onto AHC biosensors at 3 mg/ml in PBS for 300 s. A biosensor quenching step followed by the association of hu IgG Fc (Sigma Aldrich) protein at 20 µg/mL for 200 s preceded sensor rinsing in PBS for 30 s. Subsequently, association with (rh) TNFα was performed for 600 s at 100 nM, followed by another association step with either adalimumab or the cattle-derived sample for 600 s at 100 nM in the presence of 20 µg/ml hu IgG Fc. Finally, association to the secondary antibody (100 nM) was determined for 600 s in the presence of 20 µg/ml hu IgG-Fc protein (Sigma Aldrich). Each biolayer interferometry experiment included appropriate negative controls, such as an unloaded sensor control and unrelated antigens to validate specificities. The resulting data were analyzed using ForteBio data analysis software 12.2 after Savitzky–Golay filtering.

4.6 Human TNF-α HEK reporter assay

To assess the activation of the NF-κB – AP-1 pathway, the TNF-α HEK-Blue™ assay (InvivoGen) was conducted following the manufacturer's instructions.

In brief, 5×10^4 cells were seeded into a 96-well plate and stimulated with 1 ng/ml rh TNF-α, 10 min after the addition of 25 nM or 5 nM of the anti-TNF-α antibody samples, for a 24-h incubation period at 37 °C and 5 % CO_2. In parallel, cells were also incubated with identical concentrations of TNF-α, with and without anti-TNF-α sample treatment, serving as positive and negative controls, respectively.

For IC_{50} determination, samples were titrated in a 1:5 serial dilution, ranging from 500 nM to 3.3 fM, and tested in the presence of a final concentration of 1 ng/mL (rh) TNF-α. To account for background, measurements were taken for cell culture medium only. After 24 h, 20 µL of cell culture supernatants were mixed with 180 µl QUANTI-Blue medium in a fresh 96-well plate and incubated for 1 h at 37 °C and 5 % CO_2. Optical density was measured at 640 nm using a multi-mode microplate reader (Synergy HTX, BioTek), and the results were normalized to the positive control of 1 ng/ml TNF-α prior data analysis using one-way ANOVA with Dunnett's multiple comparisons test. *p*-values < 0.05 were considered statistically significant.

4.7 L929 cytotoxicity assay

To assess the inhibition of TNF-α induced cytotoxicity in L929 cells (ATCC), a neutralization assay was conducted. For this, 1×10^5 L929 cells were seeded into a black, clear-bottom 384-well micro titer plate (MTP, Greiner). After 1 h, anti-TNF-α samples were added and incubated for 15 min, followed by addition of 10 nM (rh) TNF-α and 30 nM SYTOX™ Green Dead Cell Stain (Invitrogen). Dead cell signals were measured using an IncuCyte system (Sartorius), incubating the MTP at 37 °C and 5 % CO_2. Experiments were performed with biological duplicates, and cell death was normalized to TNF-α treated cells without antibody treatment. Controls included untreated cells and staurosporine-treated cells as negative and positive controls, respectively. Data was analyzed with a variable slope four-parameter fit, and significance was determined using one-way ANOVA with Dunnett's multiple comparisons test ($p < 0.05$).

4.8 Molecular modeling

To create three-dimensional models for structural visualization, the full-length structure of adalimumab and the chimeric ultralong CDR-H3 IgG were built using the antibody modeler tool in the molecular modeling software package moe (Molecular Operating Environment 2022.02: Chemical Computing Group Inc.; 2022). Structural models of the Knobbody and engrafted knobs into the Fc CH3 AB or EF loops were built by generating models of the knobs and adding them to the different Fc regions of linkage or engraftment via moe's protein builder and linker modeler. Finally, energy minimization of all constructs was performed. Visualization of 3D structures was done with PyMOL (The PyMOL Molecular Graphics System, Version 2.5.7 Schrödinger, LLC.).

Acknowledgments: We thank Sigrid Auth, Daniel Klewinghaus, Claudia Kubis, Jennifer Schanz, Joerg Plaschke, Gernot Musch and Dirk Müller-Pompalla for discussion, and experimental and data support.
Research ethics: Not applicable.
Author contributions: The authors have accepted responsibility for the entire content of this manuscript and approved its submission.
Competing interests: Except HK all authors were or are affiliated with Merck Healthcare KGaA. Besides, this work was conducted in the absence of any commercial interest.
Research funding: Not applicable.
Data availability: The raw data can be obtained on request from the corresponding author.

References

Adams, R., Joyce, C., Kuravskiy, M., Harrison, K., Ahdash, Z., Balmforth, M., Chia, K., Marceddu, C., Coates, M., Snowden, J., et al. (2023). Serum albumin binding knob domains engineered within a VH framework III bispecific antibody format and as chimeric peptides. *Front. Immunol.* 14: 1170357.

Arras, P., Yoo, H.B., Pekar, L., Clarke, T., Friedrich, L., Schröter, C., Schanz, J., Tonillo, J., Siegmund, V., Doerner, A., et al. (2023a). AI/ML combined with next-generation sequencing of VHH immune repertoires enables the rapid identification of de novo humanized and sequence-optimized single domain antibodies: a prospective case study. *Front. Mol. Biosci.* 10: 1249247.

Arras, P., Yoo, H.B., Pekar, L., Schröter, C., Clarke, T., Krah, S., Klewinghaus, D., Siegmund, V., Evers, A., and Zielonka, S. (2023b). A library approach for the *de novo* high-throughput isolation of humanized VHH domains with favorable developability properties following camelid immunization. *mAbs* 15: 2261149.

Arras, P., Zimmermann, J., Lipinski, B., Yanakieva, D., Klewinghaus, D., Krah, S., Kolmar, H., Pekar, L., and Zielonka, S. (2023c) Isolation of antigen-specific unconventional bovine ultra-long CDR3H antibodies using cattle immunization in combination with yeast surface display. In: Zielonka, S., and Krah, S. (Eds.). *Genotype phenotype coupling, methods in molecular biology*. Springer US, New York, NY, pp. 113–129.

Bain, B. and Brazil, M. (2003). Adalimumab. *Nat. Rev. Drug Discov.* 2: 693–694.

Benatuil, L., Perez, J.M., Belk, J., and Hsieh, C.-M. (2010). An improved yeast transformation method for the generation of very large human antibody libraries. *Protein Eng. Des. Selection* 23: 155–159.

Carswell, E.A., Old, L.J., Kassel, R.L., Green, S., Fiore, N., and Williamson, B. (1975). An endotoxin-induced serum factor that causes necrosis of tumors. *Proc. Natl. Acad. Sci. U.S.A.* 72: 3666–3670.

Dakhel, S., Lizak, C., Matasci, M., Mock, J., Villa, A., Neri, D., and Cazzamalli, S. (2021). An attenuated targeted-TNF localizes to tumors in vivo and regains activity at the site of disease. *IJMS* 22: 10020.

Doerner, A., Rhiel, L., Zielonka, S., and Kolmar, H. (2014). Therapeutic antibody engineering by high efficiency cell screening. *FEBS Lett.* 588: 278–287.

Dong, J., Finn, J.A., Larsen, P.A., Smith, T.P.L., and Crowe, J.E. (2019). Structural diversity of ultralong CDRH3s in seven bovine antibody heavy chains. *Front. Immunol.* 10, https://doi.org/10.3389/fimmu.2019.00558.

Duggan, S. (2018). Caplacizumab: first global approval. *Drugs* 78: 1639–1642.

Durocher, Y. (2002). High-level and high-throughput recombinant protein production by transient transfection of suspension-growing human 293-EBNA1 cells. *Nucleic Acids Res*. 30, 9e–99.

Haakenson, J.K., Huang, R., and Smider, V.V. (2018). Diversity in the cow ultralong CDR H3 antibody repertoire. *Front. Immunol.* 9, https://doi.org/10.3389/fimmu.2018.01262.

Hawkins, A., Joyce, C., Brady, K., Hold, A., Smith, A., Knight, M., Howard, C., Van Den Elsen, J., Lawson, A.D.G., and Macpherson, A. (2022). The proximity of the N- and C- termini of bovine knob domains enable engineering of target specificity into polypeptide chains. *mAbs* 14: 2076295.

Huang, R., Warner Jenkins, G., Kim, Y., Stanfield, R.L., Singh, A., Martinez-Yamout, M., Kroon, G.J., Torres, J.L., Jackson, A.M., Kelley, A., et al. (2023). The smallest functional antibody fragment: ultralong CDR H3 antibody knob regions potently neutralize SARS-CoV-2. *Proc. Natl. Acad. Sci. U.S.A.* 120: e2303455120.

Humphreys, D.T. and Wilson, M.R. (1999). Modes of L929 cell death induced by TNF-α and other cytotoxic agents. *Cytokine* 11: 773–782.

Jang, D., Lee, A.-H., Shin, H.-Y., Song, H.-R., Park, J.-H., Kang, T.-B., Lee, S.-R., and Yang, S.-H. (2021). The role of tumor necrosis factor alpha (TNF-α) in autoimmune disease and current TNF-α inhibitors in therapeutics. *Int. J. Mol. Sci.* 22: 2719.

Keam, S.J. (2023). Ozoralizumab: first approval. *Drugs* 83: 87–92.

Klewinghaus, D., Pekar, L., Arras, P., Krah, S., Valldorf, B., Kolmar, H., and Zielonka, S. (2022). Grabbing the bull by both horns: bovine ultralong CDR-H3 paratopes enable engineering of 'almost natural' common light chain bispecific antibodies suitable for effector cell redirection. *Front. Immunol.* 12, https://doi.org/10.3389/fimmu.2021.801368.

Krah, S., Kolmar, H., Becker, S., and Zielonka, S. (2018). Engineering IgG-like bispecific antibodies – an overview. *Antibodies* 7: 28.

Li, P., Zheng, Y., and Chen, X. (2017). Drugs for autoimmune inflammatory diseases: from small molecule compounds to anti-TNF biologics. *Front. Pharmacol.* 8: 460.

Macpherson, A., Birtley, J.R., Broadbridge, R.J., Brady, K., Schulze, M.-S.E.D., Tang, Y., Joyce, C., Saunders, K., Bogle, G., Horton, J., et al. (2021a). The chemical synthesis of knob domain antibody fragments. *ACS Chem. Biol*. 16: 1757–1769.

Macpherson, A., Laabei, M., Ahdash, Z., Graewert, M.A., Birtley, J.R., Schulze, M.-S.E., Crennell, S., Robinson, S.A., Holmes, B., Oleinikovas, V., et al. (2021b). The allosteric modulation of complement C5 by knob domain peptides. *eLife* 10, https://doi.org/10.7554/eLife.63586.

Macpherson, A., Scott-Tucker, A., Spiliotopoulos, A., Simpson, C., Staniforth, J., Hold, A., Snowden, J., Manning, L., van den Elsen, J., and Lawson, A.D.G. (2020). Isolation of antigen-specific, disulphide-rich knob domain peptides from bovine antibodies. *PLoS Biol*. 18: e3000821.

Markham, A. (2022). Envafolimab: first approval. *Drugs* 82: 235–240.

Moudgil, K.D. and Choubey, D. (2011). Cytokines in autoimmunity: role in induction, regulation, and treatment. *J. Interferon Cytokine Res.* 31: 695–703.

Passon, M., De Smedt, S., and Svilenov, H.L. (2023). Principles of antibodies with ultralong complementarity-determining regions and picobodies. *Biotechnol. Adv.* 64: 108120.

Pekar, L., Klausz, K., Busch, M., Valldorf, B., Kolmar, H., Wesch, D., Oberg, H.-H., Krohn, S., Boje, A.S., Gehlert, C.L., et al. (2021a). Affinity maturation of B7-H6 translates into enhanced NK cell-mediated tumor cell lysis and improved proinflammatory cytokine release of bispecific immunoligands via NKp30 engagement. *J. Immunol.* 206: 225–236.

Pekar, L., Klewinghaus, D., Arras, P., Carrara, S.C., Harwardt, J., Krah, S., Yanakieva, D., Toleikis, L., Smider, V.V., Kolmar, H., et al. (2021b). Milking the cow: cattle-derived chimeric ultralong CDR-H3 antibodies and their engineered CDR-H3-only Knobbody counterparts targeting epidermal growth factor receptor elicit potent NK cell-mediated cytotoxicity. *Front. Immunol.* 12: 4378.

Rossotti, M.A., Bélanger, K., Henry, K.A., and Tanha, J. (2022). Immunogenicity and humanization of single-domain antibodies. *FEBS J.* 289: 4304–4327.

Roth, L., Grzeschik, J., Hinz, S.C., Becker, S., Toleikis, L., Busch, M., Kolmar, H., Krah, S., and Zielonka, S. (2019). Facile generation of antibody heavy and light chain diversities for yeast surface display by Golden Gate Cloning. *Biol. Chem.* 400: 383–393.

Saini, S.S., Allore, B., Jacobs, R.M., and Kaushik, A. (1999). Exceptionally long CDR3H region with multiple cysteine residues in functional bovine IgM antibodies. *Eur. J. Immunol.* 29: 2420–2426.

Saini, S.S., Farrugia, W., Ramsland, P.A., and Kaushik, A.K. (2003). Bovine IgM antibodies with exceptionally long complementarity-determining region 3 of the heavy chain share unique structural properties conferring restricted VH + Vλ pairings. *Int. Immunol.* 15: 845–853.

Sok, D., Le, K.M., Vadnais, M., Saye-Francisco, K.L., Jardine, J.G., Torres, J.L., Berndsen, Z.T., Kong, L., Stanfield, R., Ruiz, J., et al. (2017). Rapid elicitation of broadly neutralizing antibodies to HIV by immunization in cows. *Nature* 548: 108–111.

Stanfield, R.L., Berndsen, Z.T., Huang, R., Sok, D., Warner, G., Torres, J.L., Burton, D.R., Ward, A.B., Wilson, I.A., and Smider, V.V. (2020). Structural basis of broad HIV neutralization by a vaccine-induced cow antibody. *Sci. Adv.* 6: eaba0468.

Stanfield, R.L., Wilson, I.A., and Smider, V.V. (2016). Conservation and diversity in the ultralong third heavy-chain complementarity-determining region of bovine antibodies. *Sci. Immunol.* 1: aaf7962.

Sulea, T. (2022) Humanization of camelid single-domain antibodies. In: Hussack, G., and Henry, K.A. (Eds.). *Single-domain antibodies*. Springer US, New York, NY, pp. 299–312.

Svilenov, H.L., Sacherl, J., Protzer, U., Zacharias, M., and Buchner, J. (2021). Mechanistic principles of an ultra-long bovine CDR reveal strategies for antibody design. *Nat. Commun.* 12: 6737.

Urquhart, L. (2023). Top companies and drugs by sales in 2022. *Nat. Rev. Drug Discov.* 22: 260.

Valldorf, B., Hinz, S.C., Russo, G., Pekar, L., Mohr, L., Klemm, J., Doerner, A., Krah, S., Hust, M., and Zielonka, S. (2022). Antibody display technologies: selecting the cream of the crop. *Biol. Chem.* 403: 455–477.

Vincke, C., Loris, R., Saerens, D., Martinez-Rodriguez, S., Muyldermans, S., and Conrath, K. (2009). General strategy to humanize a camelid single-domain antibody and identification of a universal humanized nanobody scaffold. *J. Biol. Chem.* 284: 3273–3284.

Wang, F., Ekiert, D.C., Ahmad, I., Yu, W., Zhang, Y., Bazirgan, O., Torkamani, A., Raudsepp, T., Mwangi, W., Criscitiello, M.F., et al. (2013). Reshaping antibody diversity. *Cell* 153: 1379–1393.

Weaver-Feldhaus, J.M., Lou, J., Coleman, J.R., Siegel, R.W., Marks, J.D., and Feldhaus, M.J. (2004). Yeast mating for combinatorial Fab library generation and surface display. *FEBS Lett*. 564: 24–34.

Wozniak-Knopp, G., Bartl, S., Bauer, A., Mostageer, M., Woisetschläger, M., Antes, B., Ettl, K., Kainer, M., Weberhofer, G., Wiederkum, S., et al. (2010). Introducing antigen-binding sites in structural loops of immunoglobulin constant domains: Fc fragments with engineered HER2/neu-binding sites and antibody properties. *Protein Eng. Des. Sel.* 23: 289–297.

Yanakieva, D., Vollmer, L., Evers, A., Siegmund, V., Arras, P., Pekar, L., Doerner, A., Valldorf, B., Kolmar, H., Zielonka, S., et al. (2023). Cattle-derived knob paratopes grafted onto peripheral loops of the IgG1 Fc region enable the generation of a novel symmetric bispecific antibody format. *Front. Immunol.* 14: 1238313.

Supplementary Material: This article contains supplementary material (https://doi.org/10.1515/hsz-2023-0370).